Estimation of Fekete Points

E. Bendito, A. Carmona, A. M. Encinas and J. M. Gesto

e-mail: jose.manuel.gesto@upc.edu

Departament de Matemàtica Aplicada III

Universitat Politècnica de Catalunya. España

Abstract

In this paper we present a procedure for the numerical estimation of the Fekete points of a wide variety of compact sets in $\mathbb{R}^3$. We understand the problem of the Fekete points in terms of the identification of nearly equilibrium configurations for a potential energy that depends on the relative position of N particles.

The compact sets for which our procedure has been designed can be described basically as the finite union of piecewise regular surfaces and curves. To determine a good configuration to start the search of the Fekete points of these objects, we construct a sequence of approximating regular surfaces. Our algorithm is based in the concept of disequilibrium degree, defined from a physical interpretation of the behavior of a system of particles when they search for a minimal energy configuration. Moreover, the algorithm is efficient and robust independently of the compact set considered as well as of the kernel used to define the energy. The numerical experimentation suggests that a nearly optimal configuration can be obtained by means of the procedure introduced here with a total computational cost of order less than N^3.

1 Introduction

The problem of obtaining the Fekete points of a compact set has filled a pre-eminent place in the mathematical research along the last decades. In its original version, the problem consists in determining the position of N points of a compact subset $S \subset \mathbb{R}^2$ that maximize the product of its mutual Euclidean distances. The N-tuples, $\omega_N = \{x_1, \ldots, x_N\}$, that satisfy this property are the so-called *N-th order Fekete points* of S. It is not difficult to check that these N-tuples minimize in S the functional

$$\mathcal{I}(\omega_N) = \sum_{1 \leq i < j \leq N} \mathcal{K}(x_i, x_j), \tag{1}$$

where $\mathcal{K}(x_i, x_j) = -\ln |x_i - x_j|$ is the so-called *logarithmic kernel* and $|x_i - x_j|$ is the Euclidean distance between x_i and x_j. The value $\mathcal{I}(\omega_N)$ represents the *potential energy* corresponding

to the logarithmic kernel when a unitary weight is associated with any point. In the three-dimensional Euclidean space multiple variants of the problem can be formulated by considering different kernels, among which the *Riesz's kernels*, defined by $\mathcal{K}(x_i, x_j) = |x_i - x_j|^{-s}$ with $s > 0$, constitute a family of special interest. In particular, the *Newtonian kernel*, obtained taking $s = 1$, has become the most relevant case and its potential energy $\mathcal{I}(\omega_N)$ is named *electrostatic potential energy*. For a more detailed description of this topic, see for instance [13].

The determination of the Fekete points of the unit sphere is considered a model of highly non-linear optimization problem with non-linear constraints. In fact, obtaining a robust and efficient algorithm for that problem still constitutes a challenge in computational mathematics [20]. In general, only when the constraints are linear or they can be sufficiently well approximated by linear constraints it is reasonable to expect a good behavior of the usual algorithms for optimization problems with constraints. However, even in this case, the convergence ratios result lower than the ones corresponding to free optimization methods. Some authors choose to transform problems like the Fekete points one in optimization problems without constraints by considering a parametrization of the surface [15, 23]. In this way, they can use classical optimization techniques such as the *Gradient Method*, the *Conjugate Gradient Method*, the *Newton Method* and the family of *quasi-Newton methods*. Also other methods like the so-called *Combinatory Optimization methods* have been used, among which they stand out the *Simulated Annealing*, *Tabu Search* and *Genetic Algorithms* [15]. On the other hand, estimations of the Fekete points of the torus have been recently studied, see [9]. With regards to non-regular geometries, the Fekete points of the triangle have been analyzed due to its usefulness in numerical interpolation, see [8, 10, 21].

A considerable amount of theoretical and numerical results have been obtained related to the different versions of Fekete points problem, see for instance [9, 11, 12, 15, 17, 18, 21, 23], and it has been completely solved in some particular cases. Nevertheless, it is widely recognized that the simple obtaining of a position near to a local optimum for hundreds of points in the sphere requires to dispose of an important calculation infrastructure. The possibility of obtaining good configurations of thousands of points by reducing the number of unknowns by means of symmetries has been raised, see [9].

In this paper we propose an algorithm for the numerical estimation of the Fekete points of non-smooth compact sets. Essentially, these compact sets are the finite union of piecewise regular manifolds of different dimensions. We focus in the three-dimensional case, since the estimation of Fekete points is of interest in Chemistry, Biology, Nanotechnology, CAD, etc, see [1, 2, 9, 18]. On the other hand, in the examples that we present here we have considered the *Newtonian kernel* due to its special relevance, for instance in the electrical and gravitational phenomena. Moreover, the relation between the electrostatic potential energy of a system of particles and the energy of a distributed charge has been analyzed by several authors, see [11], whose work will provide us a good framework for the contrast of the quality of the solutions obtained with our algorithm.

We start describing an algorithm for the estimation of the Fekete points of smooth surfaces. After that, we analyze the behavior of this algorithm with the prototype problem,

the unit sphere. Then, we present a transition case: we estimate the Fekete points of the unit cube by means of this algorithm for smooth surfaces. It requires the use of symmetries to reduce the domain of analysis to an open triangle. Finally, we develop a strategy for the estimation of the Fekete points of non-smooth surfaces, and we present several examples.

2 Smooth Surfaces

In this section we present the fundamentals of an algorithm to obtain good estimations of the Fekete points of a smooth surface. The basic structure of the algorithm is classical: each iteration consists in obtaining the advance direction and the step size in a deterministic way.

The ideas behind the algorithm come from Physics. We do not try to answer directly the question about which are the minimum potential energy configurations, but how the points of a non-optimal configuration can advance, in a mechanical sense, to reach a minimum potential energy configuration. The equivalence between minimum potential energy and static stable equilibrium configurations constitutes the key of the method. A mechanical system formed by particles is in equilibrium if the total force that acts on each one of these particles is null. The equilibrium is stable if small perturbations in the position tend to return each particle to its original position, and then this position is a minimum for the potential energy of the system. So, for a given non-optimal configuration, non-equilibrated forces must be acting on the particles and these forces will inevitably induce its movement. We wonder about the character of these forces and this movement and about when they will carry the particles to an equilibrium position.

Firstly note that the energy of a system of N unitary particles at $x_k \in \mathbb{R}^3$, $k = 1, \ldots, N$, is given by $\mathcal{I} = \frac{1}{2}\sum_{i=1}^{N} V_i$, where $V_i = \sum_{\substack{j=1 \\ j\neq i}}^{N} \mathcal{K}(x_i, x_j)$ is the potential created at x_i by all the other particles. If the particles lie on a regular surface $S \subset \mathbb{R}^3$, then any point $x_i \in S$ has assigned a normal vector n_i. If we fix the position of the $N-1$ particles $\{x_j \in S : j = 1, \ldots, N, j \neq i\}$, V_i is a function of x_i and the opposite of its gradient, that we denote by $F_i = -\nabla V_i \in T_{x_i}(\mathbb{R}^3)$, represents the repulsive force that acts on the i-th particle due to the existence of the rest. We consider $F_i^n = \langle F_i, n_i\rangle n_i$ and $F_i^T = F_i - F_i^n$, the *normal* and *tangent components* to S of the force F_i at x_i, respectively. On the other hand, if $M = S^N$, then $\left(F_1^T, \ldots, F_N^T\right) = -\nabla \mathcal{I}_{|M}$ is the direction of maximum descent of $\mathcal{I}$ in M, independently of the possible parametrizations of S.

The i-th particle is in *equilibrium* on S if $F_i^T = 0$. Therefore, $|F_i^T|$ could be a measure of the disequilibrium degree of that particle on S. Nevertheless, Fig. 1 suggests that an alternative measure of the disequilibrium degree based on the angle between F_i and n_i could result more satisfactory. Effectively, two particles x_i, x_j with $|F_i^T| = |F_j^T|$ can be "more or less equilibrated" on S depending on the angle between the forces F_i and F_j and its corresponding normal vectors n_i and n_j. We define $\dfrac{|F_i^T|}{|F_i|}$ as the *disequilibrium degree* of the

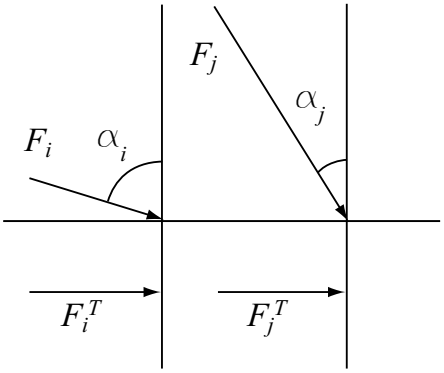

Figure 1: Disequilibrium degree.

i-th particle. The suitability of this choice will be showed clearly throughout the paper.

The following simple proposition establishes that to advance according with this disequilibrium measure descents the energy of the system.

Proposition 2.1 *The direction*

$$w = \left(\frac{F_1^T}{|F_1|}, \ldots, \frac{F_N^T}{|F_N|} \right)$$

is of descent of the energy constrained to M. In addition, every particle contributes to the descent.

Proof. The direction w is obviously compatible with the constraints of the problem, since $w \in T_x(M)$. The result follows from the fact that

$$\langle w, -\nabla \mathcal{I}_{|M} \rangle = \sum_{i=1}^{N} \frac{|F_i^T|^2}{|F_i|} \geq 0. \quad \blacksquare$$

Observe that the direction w does not coincide with the one given by the Gradient method except in very particular cases, for example in the sphere with a great number of particles when they are in stages very close to the equilibrium. The rest of classical optimization methods, like Conjugate Gradient, Newton or quasi-Newton, choose advance directions that in general do not guarantee that each particle contributes to the descent, which results not very natural in the iterative process. On the other hand, as the disequilibrium degree indicator that we propose here is bounded -in fact, normalized between 0 and 1-, it allows to treat each particle only in relation to its own potential equilibrium degree and independently of the relative distance to the rest of particles.

In any case, the more substantial difference between our approach and classical methods is that the determination of the advance direction and the step size is completely independent

of the parametrization that has been chosen for the surface S. Regarding to the direction, that independence has already been made clear. As for the step size some considerations must be made. Given an initial configuration, a unique stationary point for $\mathcal{I}$ must exist such that the particles arrive to it following the direction $w_i = \dfrac{F_i^T}{|F_i|}$. Consequently, from the point of view of Mechanics, these directions not only can be understood as energy descent directions, but also as the velocity fields of the paths described by the particles in its movement towards the equilibrium. This approach allows us to look at the optimization problem from the dynamic systems perspective. The step size will be chosen by applying an explicit forward Euler method to the system of ODE whose solutions are precisely these paths. These ODE are raised in a natural way in the coordinates of the ambient space and its numerical integration fixes a displacement for each particle in that space. In general, the application of that displacement takes the particles out of the surface S, which generates the need of considering an algorithm to return the particles to the surface in each iteration. Maybe the most versatile and simple one consists in using the gradient field of an implicit representation of the surface. When the surface is described in a parametric form, the composition with the metric allow us to transfer to the parametric space the magnitude of the step to apply, which solves the return problem.

It is interesting to make some observations about the treatment of the problem from this mechanical point of view. If $x(t) = (x_1(t), \dots, x_N(t))$ denotes the position of N particles in the instant t, then an equation for the movement of the system on a surface S can be

$$x''(t) = -\nabla\mathcal{I}(x(t)) - cx'(t) + \Phi(x(t), x'(t)). \tag{2}$$

The term $-cx'(t)$, with $c > 0$, represents a dissipative force of viscous nature and $\Phi = (\Phi_1, \dots, \Phi_N)$ is an additional force that takes into account the interaction between each particle and S. For each $i = 1, \dots, N$, the normal component of Φ_i, $\Phi_i^n = \rho\,|x_i'|^2 - F_i^n$, cancels the normal component of F_i and it provides the centripetal force, being ρ the normal curvature in the direction of x_i' at $x_i \in S$. The tangent component Φ_i^T considers the friction with S and its expression depends on each particular model. If the friction force is not considered, then it is easy to prove that as $c \to \infty$ the trajectories that solve (2) tend to be the enveloping of the vectors F_i^T. Hence, in this case the particles follow the direction of $-\nabla\mathcal{I}_{|M}$. It is possible to propose a friction model such that the corresponding trajectories tend to be the enveloping of the vectors w_i.

Therefore, the search for the minimum of the energy will be carried out by obtaining the paths described by the particles in its movement towards the equilibrium. These ideas belong to the fundamentals of Rational Mechanics and have already been used in the literature by different authors, see for example [16, 19, 22]. However, in many cases the equilibrium of the particles is purely heuristic and it does not come from the minimization of an explicit functional, and, anyway, the objective is not to localize an equilibrium configuration as a goal in itself, but to arrive to a reasonable level of approximation.

In short, the system of ODE to solve is

$$x' = w. \tag{3}$$

For its numerical resolution we will use the following explicit forward Euler method:

$$x^{k+1} = x^k + a\,\varphi(x^k)\,w^k \tag{4}$$

where a is a positive scalar that depends on the kernel and on the surface S, and $\varphi(x^k)$ depends on the current position of all the particles of the system and allows us to adapt the step size to the difficulty of the different configurations that appear during the calculation. The step size must be reduced when there exist very close particles in order that they do not "run helter-skelter" breaking the continuity of the movement, whereas if the relative distances grow, the step size can be increased in benefit of the convergence ratio. An appropriate choice is

$$\varphi(x) = \min_{1\le p<q\le N}\{|x_p - x_q|\},$$

according to which $a\,|w_i|$ represents the fraction of the minimum distance between particles that the i-th one advances in each iteration.

The numerical experimentation carried out by the authors confirms that this algorithm converges -in the sense that it localizes an equilibrium position- even for crazy initial positions, for instance the corresponding to confine the N particles in the N-th part of the area of the surface.

3 Unit Sphere

The problem of obtaining Fekete points in the unit sphere is probably the most characteristic both for its hardness ([20]) and for its different applications. From a numerical point of view we can mention the Ph.D. of Y. Zhou [23] and some works generated around it [17, 18]. In that Ph.D. minimum energy configurations are presented for each $N \le 200$ for the Newtonian and logarithmic kernels. The algorithms used were quasi-Newton after the elimination of the constraints by means of the stereographic projection. In view of these results and other ones of theoretical character, extrapolation formulae for the minimum energy associated to those kernels in the sphere were proposed. Recently, some works have appeared in which good configurations of 1600 points obtained by means of *ad hoc* algorithms are presented, see [9].

For the unit sphere, after the generation of an arbitrary initial configuration x^0 of N different points, the k-th iteration of our algorithm simply consists in:

-Calculate the advance direction w^{k-1}.

-Calculate $\hat{x}^k = x^{k-1} + a\,d_{k-1}\,w^{k-1}$.

-Obtain the k-th configuration: $x_i^k = \dfrac{\hat{x}_i^k}{|\hat{x}_i^k|}$.

Here, d_{k-1} represents the minimum distance between two points of the $(k-1)$-th configuration, that is obtained as a byproduct of the advance direction calculation. It is necessary

to indicate that, for the kernels we are interested in, the most expensive step of the iterative process is precisely the calculation of this direction, that involves N^2 operations. In Table 1 we show reference values for the coefficient a for some kernels in the sphere.

Kernel	Logarithmic	Newtonian	Riesz $s = 2$	Riesz $s = 3$
a	8	1	0.1	0.02

Table 1: Reference values for the coefficient a.

To study the convergence of our algorithm, we use $\max_{1\leq i\leq N} |w_i|$; *i.e.*, the maximum disequilibrium degree of the particles, as a measure of the error. If we analyze the evolution of the error with respect to the iteration number, we observe that a linear convergence ratio is systematically attained after a first highly non-linear stage. When the linear stage is reached the particles can be supposed to be sufficiently close to a stationary point, in the sense that from this moment the Newton algorithm can be used with guaranty of convergence. Figure 2 (a) illustrates the behavior of the error for a configuration of 1000 particles with the Newtonian kernel.

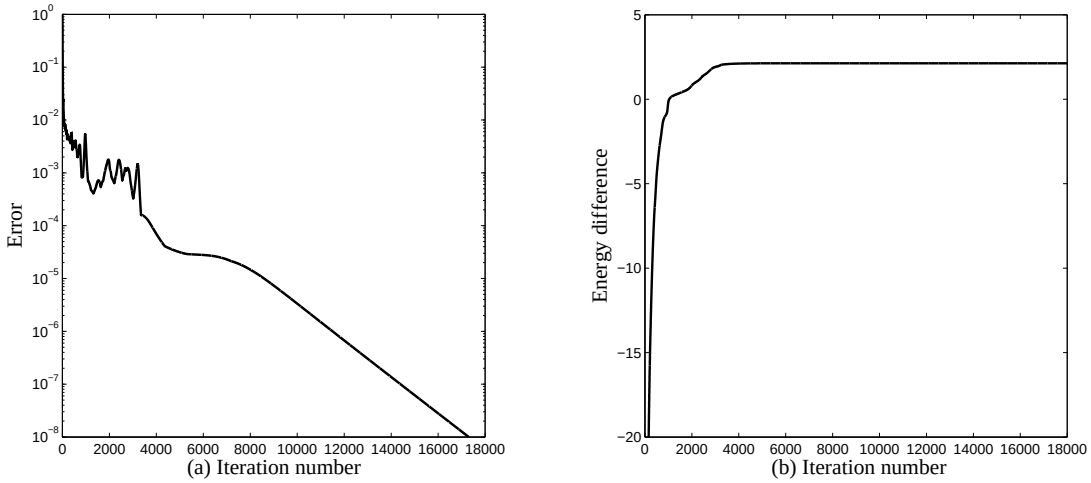

Figure 2: The behavior of the algorithm.

Figure 2 (b) displays the evolution of the difference between the energy corresponding to the extrapolation formula given in [23] and the energy computed with our algorithm. We must note that the energy given by the formula, in spite of been accurate, can be improved very quickly. In fact, this happens long before the linear tendency is reached. Figure 3 shows the initial and final configurations of the non-linear stage for the previous case as well as the Dirichlet cells of both configurations. The initial configuration was generated randomly by adjusting the distribution of the particles to a uniform probability density on the sphere. We must note that the energy produced by the initial configuration is 500144.450659, and after the iterative process the energy value is 482534.789049, which represents only a 3.5% of decrease. On the other hand, the algorithm shows a high efficiency, since the time required

to reach the linear tendency was around 15 minutes and to surpass the extrapolated energy value required only around 2 minutes with a conventional Pentium IV processor of 2.54 GHz and 512 Mb of RAM.

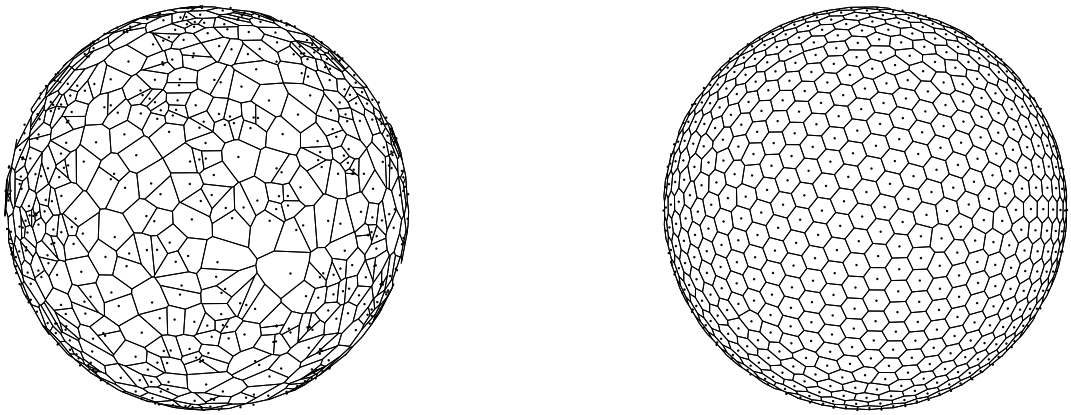

Figure 3: 1000 particles and its Dirichlet cells for the iterations 0 and 8000.

Figure 4 shows a configuration of 5000 particles when the linear tendency has been attained, which required approximately 20 hours of calculation time. With a configuration of 50000 particles, and without considering any kind of symmetry, the time required to improve the energy corresponding to the extrapolation formula was of approximately 15 hours.

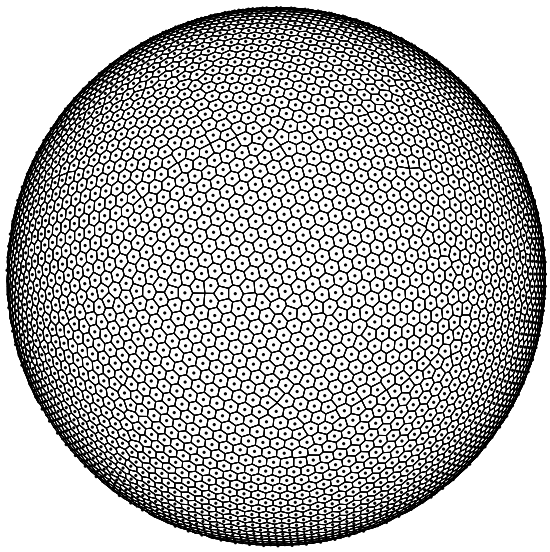

Figure 4: A beautiful configuration and the Dirichlet cells for $N = 5000$.

Although to extract definitive conclusions about the computational cost of the algorithm is not possible yet, the obtained results allow us to be optimistic in that sense, and they seem to suggest an average cost of order less than N^3 for obtaining a near-equilibrium

configuration. It must be considered that in such a non-linear problem, some fluctuations in the cost are natural. For instance, for fixed N similar initial configurations could require different calculation times, whereas configurations with more particles than others could require less iterations. It is clear that the memory requirements are of order N. Moreover, the tests realized until now confirm the robustness of the algorithm.

To obtain good equilibrium configurations for a great number of particles without an increase of the calculus infrastructure, we can use the symmetries of the sphere. The geodesic grids are good initial configurations that take into account that symmetries. In particular, we consider families of truncated icosahedron, which corresponds to use 120 symmetries. Although the geodesics constitute an excellent family of initial configurations, they do not present a uniform density of points. This is due to the projection that takes the points from the faces of the icosahedron to the sphere. In this conditions our algorithm basically smooths the density, as can be seen in Figure 5. In this figure we represent the initial and final positions of the points corresponding to a face of the original icosahedron for a configuration with 12002 particles in total.

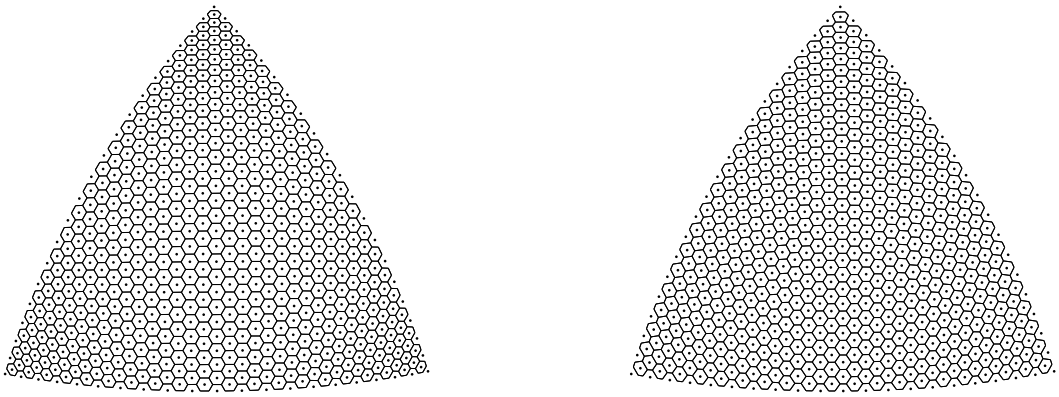

Figure 5: Initial and final configurations in a spherical triangle.

In Figure 6 we present the convergence evolution for several configurations whose initial positions are defined by different frequency geodesic grids. The total number of particles for each one of the seven cases considered are: (1) $N = 4322$, (2) $N = 12002$, (3) $N = 27002$, (4) $N = 52922$, (5) $N = 100922$, (6) $N = 201722$, (7) $N = 300002$. Note that the evolution of the error is very smooth even before the final linear tendency is attained. A reason for that is the great quality of the initial configurations. Moreover, it must be observed that all the geodesics of this family start with approximately the same error. This fact can be used to realize an analysis of the cost in similar conditions. If we consider the reference error $\mathsf{e} = 5 \cdot 10^{-3}$, we can obtain in each case the number of iterations needed to attain e. This is showed in Figure 6 as well as a simple interpolation of the data.

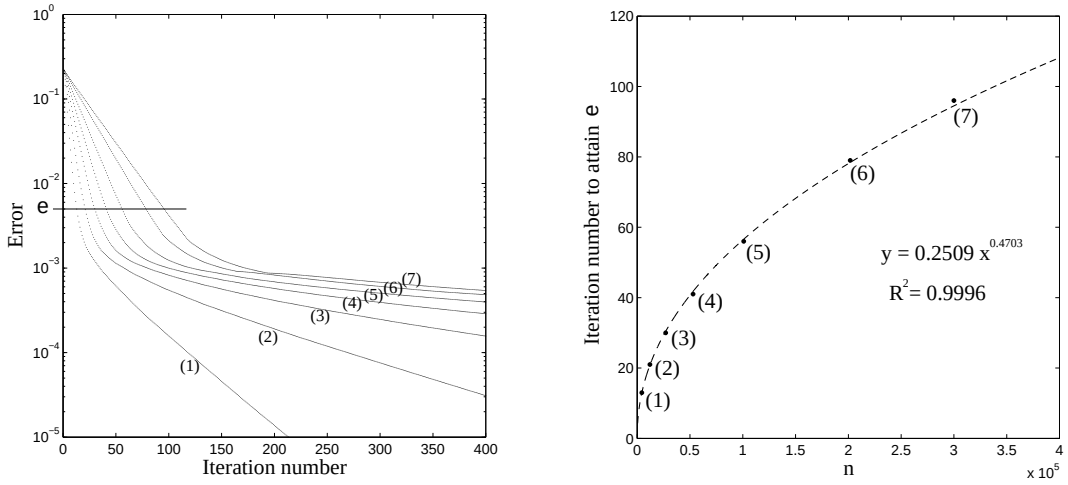

Figure 6: The behavior of the algorithm with geodesics.

4 A Transition Case

In this section we present a case that reproduces the transition between the uniform electrostatic charge density of a sphere and the asymptotic density of a cube. It is evident that the cube is not a smooth surface. Nevertheless, we have considered its 48 symmetries reducing the domain to an open triangle representing the eighth part of the cube face. An important accumulation of particles near the edges would occur, which *a priori* seems to increase the difficulty of the search of an equilibrium configuration. However, we want to emphasize that the behavior of our algorithm in the cube is essentially the same than in the sphere, and this is fundamentally due to the choice of w as advance direction. Other possible choices, as for example $\breve{w}_i = \dfrac{F_i^T}{|F_j|_{max}}$, which is equivalent to follow the gradient direction, clearly leads to unsatisfactory results.

Figure 7 shows a near-equilibrium distribution in a face of the unit cube for a total quantity of 47520 particles, which corresponds to 990 particles inside of the reference triangle. The linear tendency is reached at iteration 40000, approximately.

Clearly, the equilibrium configuration showed in Figure 7 cannot be presented as a good estimation of the Fekete points of a cube. The use of symmetries implies certain constraints. In our starting position, we have placed all the particles in the interior of the open triangle used as reduced domain, and hence in the final configuration there are no points on the edges of the cube. If we want that there are charges on the edges in the final configuration, we must to decide how many charges we have to place on the boundary of the triangle in the starting position. So, it seems necessary to complete the above algorithm to tackle the problem of the numerical estimation of the Fekete points of non-regular objects.

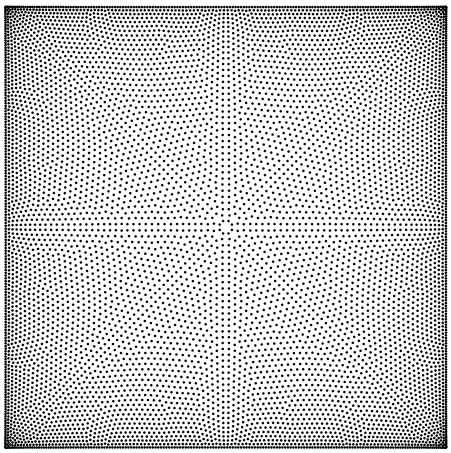

Figure 7: 7920 particles in linear tendency on a cube face.

5 Non-Smooth Surfaces

When $\mathcal{S}$ is not a connected compact differentiable surface without boundary, to estimate its Fekete points becomes a more difficult problem. For instance, if we consider $\mathcal{S}$ the boundary of a regular tetrahedron and we give an initial distribution of particles on $\mathcal{S}$, it is easy to see that the force that acts on each particle makes it remain on the face where it was initially. Therefore, if the initial distribution did not have a suitable number of particles on each face, the local minimum attained will be very far from being an acceptable solution for the global Fekete points problem on $\mathcal{S}$. In more general cases, to advance according to the direction of F_i restricted to a non-regular surface could allow the transition from one face to the other, but even then there could exist a lot of unsatisfactory local minima if the initial distribution is not suitable.

In general, for a given non-regular surface it is impossible to predict the number of particles that will lie on each face and on each edge when the Fekete problem has been solved. From a numerical point of view, one cannot expect to solve the problem beyond obtaining a local minimum from a given initial configuration. Therefore, it is necessary to design a strategy for the generation of good initial configurations. With this aim, we work from the intuitive idea that a configuration of N points in a reasonably good equilibrium state on a regular surface S_m that is sufficiently close to the non-regular surface $\mathcal{S}$ can be used to construct a good initial position to start the numerical search of the Fekete points of $\mathcal{S}$. In fact, our numerical strategy for the generation of initial positions consists in finding a sequence of acceptable equilibrium configurations on a small number of approximating regular surfaces S_k, $1 \leq k \leq r$ -we usually take $r = 2$- by means of the algorithm presented in Section 2. Each one of the points x_i of the final configuration in S_k is projected to the surface S_{k+1} to act as its starting configuration. Projecting the final r-th configuration to $\mathcal{S}$ we obtain a good starting position for a further accurate calculation of an equilibrium configuration on it. With respect to the initial configuration corresponding to S_1, there are

not special requirements and it can be generated, for instance, randomly.

In the following subsections we examine the more relevant aspects of the above reasonings. Firstly, we describe the family of compact sets where we are going to consider the Fekete points problem, and that we call *weakly smooth compact sets*, *W-compact sets* in short. We also analyze the accessibility to these compact sets by means of approximating regular surfaces, and make certain theoretical considerations that supports our numerical approach. Secondly, the foundations of a versatile technique for the generation of sequences of regular surfaces tending to W-compact sets are presented. We finish studying the potential energy restricted to a W-compact set and describing our algorithm for the estimation of the Fekete points of W-compact sets.

5.1 W-compact sets

We would like to emphasize the generality of the sets where we can obtain good configurations for the Fekete points problem; *i.e,* nearly optimal configurations for the potential energy. The more relevant characteristic of the family of sets that we consider is, roughly speaking, the piecewise smoothness in a wide sense. In particular, we admit the finite union of surfaces with curves.

Let $\mathcal{S} \subset \mathbb{R}^3$ be a connected compact set with 2-dimensional Lebesgue measure. Let us also consider the subsets

$$A = \{x \in \mathcal{S} : \mathcal{S} \text{ is a differentiable 2-manifold at } x\},$$

and

$$B = \{x \in \mathcal{S} \setminus A : \mathcal{S} \setminus A \text{ is a differentiable 1-manifold at } x\}.$$

We call *face*, *edge* and *vertex* of $\mathcal{S}$ to each connected component of A, B and $\mathcal{S} \setminus (A \cup B)$, respectively. We say that $\mathcal{S}$ is a *W-compact set*, when it has a finite number of faces, edges and vertices and in addition $\mathcal{S} \setminus A$ is a set with 1-dimensional Lebesgue measure and $\mathcal{S} \setminus (A \cup B))$ has null Lebesgue measure.

We will work with W-compact sets such that for each $n \geq m_0$ the number of connected components of $D_n = \left\{x \in \mathbb{R}^3 : d(x, \mathcal{S}) = \frac{1}{n}\right\}$ remains constant and equals the number of connected components of $\mathbb{R}^3 \setminus \mathcal{S}$, where d represents the Euclidean distance in $\mathbb{R}^3$. Then, there exists a sequence of connected compact differentiable surfaces without boundary, $\{S_n\}_{n=1}^{\infty}$, that tends to $\mathcal{S}$, in the sense that for each $x \in \mathcal{S}$, $d(x, S_n) \to 0$ and also the sequence $\left\{\max_{x \in S_n}\{d(x, \mathcal{S})\}\right\}_{n=1}^{\infty} \to 0$.

Observe that the surfaces S_n can be built from D_n by connecting all its connected components and smoothing the final surface. Specifically, the connection of two components can be made as follows. Let us consider a regular point x on a face such that x belongs to the boundary of two connected components of $\mathbb{R}^3 \setminus \mathcal{S}$. Then we can choose r_n such

that $D_n^1 = \left\{ x \in \mathbb{R}^3 : d(x, \mathcal{S}_n^1) = \dfrac{1}{n} \right\}$ has one connected component less than D_n, where $\mathcal{S}_n^1 = \mathcal{S} \setminus \{B(x, r_n) \cap \mathcal{S}\}$.

Now, we can analyze the construction of good initial positions for the Fekete points problem for W-compact sets. It is well-known that if a compact set $K \subset \mathbb{R}^3$ is the intersection of a decreasing sequence of compact sets $\{K_n\}_{n=1}^{\infty}$, then the measures that minimize the Newtonian energy of K_n vaguely converge to the measure that minimizes the Newtonian energy of K. Taking into account that the Newtonian optimal measure of K_n has its support on the outer boundary $\partial_0 K_n$, then the electrostatic optimal measures of the boundaries $\partial_0 K_n$ converge to the electrostatic optimal measure of $\partial_0 K$. On the other hand, the discrete measure supported by the Fekete points of $\partial_0 K_n$ vaguely converges to the optimal measure of $\partial_0 K_n$.

These results suggest that a sufficiently well equilibrated configuration of N points on a sufficiently good approximating surface can be used to construct a good initial position to start the search of the N-th order Fekete points of $\mathcal{S}$. Our intention here is to show numerical evidence of the effectiveness of this numerical approach even in contexts that are not necessarily under the hypotheses of the classical theorems. For other results of approximation of solutions of the energy minimization problem considering several kernels, measures sets and support spaces see [3, 7, 13]

5.2 Regular approximation to W-compact sets

From a practical point of view, we need to dispose of an effective technique to construct a sequence of approximating surfaces $\{S_n\}_{n=1}^{\infty}$ of a given W-compact set. Among the different procedures that could be used, we want to mention one based on a technique of composition of implicit functions widely used in different areas, especially in Computer Graphics, see for instance [4]. This method provides global implicit equations to describe very general geometries.

We present here a systematic analysis of three fundamental cases associated to the approximation of boundaries of open sets, surfaces with boundary and curves. Over this basis, the feasibility of the approximation of a wide variety of W-compact sets combination of these three cases by means of more general composition operations can be easily proved.

5.2.1 Case 1: Boundaries of Open Sets

Next we analyze the approximation process to the boundaries of open sets that can be described in the form

$$\Omega = \left\{ x \in \mathbb{R}^3 : \max_{1 \le i \le k} \{F_i(x)\} < 1 \right\},$$

where $F_i : \mathbb{R}^3 \longrightarrow \mathbb{R}^+$, $i = 1, \ldots, k$, $k \in \mathbb{N}$ are sufficiently smooth functions. Let we consider the sequence $\{A_n\}_{n=1}^{\infty}$ of open sets defined for each $n \in \mathbb{N}$ by

$$A_n = \left\{ x \in \mathbb{R}^3 : \sum_{i=1}^{k} F_i(x)^n < 1 \right\}.$$

Lema 5.1 *The sequence $\{A_n\}_{n=1}^{\infty}$ increases to Ω, that is, $A_n \uparrow \Omega$. Moreover, the sequence $\{\partial A_n\}_{n=1}^{\infty}$ tends to $\partial\Omega = \left\{ x \in \mathbb{R}^3 : \max_{1 \le i \le k}\{F_i(x)\} = 1 \right\}$.*

Proof. Let us consider $x \in A_n$. Then for each $i \in \{1, \ldots, k\}$, $0 \le F_i(x) < 1$, and hence $\sum_{i=1}^{k} F_i(x)^{n+1} < \sum_{i=1}^{k} F_i(x)^n < 1$ and $x \in A_{n+1}$. On the other hand, if $x \in \Omega$ and $\Phi_x = \max_{1 \le i \le k}\{F_i(x)\}$, then $0 \le \Phi_x < 1$ and $\sum_{i=1}^{k} F_i(x)^{\ell} \le k\,\Phi_x^{\ell}$, $\ell \in \mathbb{N}$. Therefore, if $n_x = \min\{j \in \mathbb{N} : k\,\Phi_x^j < 1\}$ then for each $n \in \mathbb{N}$ such that $n \ge n_x$, $x \in A_n$. ∎

The following simple example illustrates this case. The sequence of sets

$$\partial A_n = \{(x, y, z) \in \mathbb{R}^3 : x^{2n} + y^{2n} + z^{2n} = 1\},$$

goes from the sphere to the cube

$$\partial\Omega = \{(x, y, z) \in \mathbb{R}^3 : \max\{x^2, y^2, z^2\} = 1\},$$

when n goes from 1 to ∞.

5.2.2 Case 2: Surfaces with Boundary

We consider now the approximation to connected compact surfaces with boundary that can be described in the form

$$\Gamma = \left\{ x \in \mathbb{R}^3 : F(x) = 0,\ G(x) \le 0 \right\},$$

where $F, G : \mathbb{R}^3 \longrightarrow \mathbb{R}$ are sufficiently smooth functions. Consider also the sequence $\{A_n\}_{n=1}^{\infty}$ of open sets defined for each $n \in \mathbb{N}$ by

$$A_n = \left\{ x \in \mathbb{R}^3 :\ nF(x)^2 + G(x) > 0 \right\}.$$

Lema 5.2 *The sequence $\{A_n\}_{n=1}^{\infty}$ increases to $\mathbb{R}^3 \setminus \Gamma$. Moreover, the sequence $\{\partial A_n\}_{n=1}^{\infty}$ tends to Γ.*

Proof. If $x \in A_n$, then $(n+1)F(x)^2 + G(x) \geq nF(x)^2 + G(x) > 0$ and hence $x \in A_{n+1}$. On the other hand, if $x \in \mathbb{R}^3 \setminus \Gamma$ then either $F(x)^2 > 0$ or $G(x) > 0$. In any case, if $n_x = \min\left\{j \in \mathbb{N} : jF(x)^2 > -G(x)\right\}$ then for each $n \in \mathbb{N}$ such that $n \geq n_x$, $x \in A_n$. ∎

Observe that $\partial\Gamma \subset \partial A_n$ for each $n \in \mathbb{N}$. In addition, if Γ is a surface without boundary of the form $\Gamma = \left\{x \in \mathbb{R}^3 : F(x) = 0\right\}$, the above result is also true taking $G = -1$.

As an example of this situation, we can mention the approximation of the unit disc

$$\Gamma = \{(x, y, z) \in \mathbb{R}^3 : \ z = 0, \ x^2 + y^2 - 1 \leq 0\},$$

by means of the sequence of oblate ellipsoids

$$\partial A_n = \{(x, y, z) \in \mathbb{R}^3 : \ nz^2 + x^2 + y^2 - 1 = 0\}.$$

5.2.3 Case 3: Curves with Boundary

We focus here in the approximation to connected compact curves with boundary that can be described in the form

$$C = \left\{x \in \mathbb{R}^3 : F(x) = 0, \ G(x) = 0, \ H_1(x) \leq 0, \ H_2(x) \leq 0\right\},$$

where $F, G, H_1, H_2 : \mathbb{R}^3 \longrightarrow \mathbb{R}$ are sufficiently smooth functions verifying that the set $\left\{x \in \mathbb{R}^3 : H_1(x) > 0, \ H_2(x) > 0\right\}$ is empty. Consider also the sequence $\{A_n\}_{n=1}^{\infty}$, of open sets defined for each $n \in \mathbb{N}$ by

$$A_n = \left\{x \in \mathbb{R}^3 : nF(x)^2 + nG(x)^2 - H_1(x)H_2(x) > 0\right\}.$$

Lema 5.3 *The sequence $\{A_n\}_{n=1}^{\infty}$ increases to $\mathbb{R}^3 \setminus C$. Moreover, the sequence $\{\partial A_n\}_{n=1}^{\infty}$ tends to C.*

Proof. If $x \in A_n$, then

$$(n+1)F(x)^2 + (n+1)G(x)^2 - H_1(x)H_2(x) > nF(x)^2 + nG(x)^2 - H_1(x)H_2(x) > 0$$

and hence $x \in A_{n+1}$. On the other hand, if $x \in \mathbb{R}^3 \setminus C$ then either $F(x)^2 + G(x)^2 > 0$ or $H_1(x)H_2(x) < 0$. In any case, if $n_x = \min\left\{j \in \mathbb{N} : j\Big(F(x)^2 + G(x)^2\Big) > H_1(x)H_2(x)\right\}$ then $x \in A_n$, for each $n \in \mathbb{N}$ such that $n \geq n_x$. ∎

Observe that $\partial C \subset \partial A_n$ for each $n \in \mathbb{N}$. Moreover, if $\partial C = \emptyset$ it suffices to take $H_1 = H_2 = -1$, whereas if $\partial C \subset \{H_1 = 0\}$, it suffices to take $H_2 = -1$.

The approximation of the segment

$$C = \{(x, y, z) \in \mathbb{R}^3 : y = 0, \ z = 0, \ x - 1 \leq 0, \ -x - 1 \leq 0\},$$

by means of the sequence of prolate ellipsoids

$$\partial A_n = \{(x, y, z) \in \mathbb{R}^3 : ny^2 + nz^2 + x^2 - 1 = 0\},$$

illustrates this case.

5.3 The energy restricted to a W-compact set

Let $\mathcal{S}$ be a W-compact set. For each $x \in \mathcal{S}$, we can consider the set $\mathcal{C}_x$ of all the differentiable curves contained in $\mathcal{S}$ with origin in x. In this conditions, we define the *mobility set* of x on $\mathcal{S}$, $\mathcal{T}_x(\mathcal{S})$, by

$$\mathcal{T}_x(\mathcal{S}) = \left\{ \mathsf{t} \in \mathbb{R}^3 : \mathsf{t} \text{ is the unitary tangent vector at } x \text{ of } \gamma \in \mathcal{C}_x \right\}.$$

If x belongs to a face of $\mathcal{S}$, then the vectors of its mobility set generate the plane tangent to $\mathcal{S}$ at x, $T_x(\mathcal{S})$.

If $f : \mathbb{R}^3 \longrightarrow \mathbb{R}$ is a regular function in $x \in \mathcal{S}$, let us consider the scalar

$$p = \max_{\mathsf{t} \in \mathcal{T}_x(\mathcal{S})} \{-\langle \nabla f(x), \mathsf{t} \rangle\},$$

and the set $\mathsf{t}_x(\mathcal{S})$ defined by

$$\mathsf{t}_x(\mathcal{S}) = \begin{cases} \{\mathsf{t} \in \mathcal{T}_x(\mathcal{S}) : -\langle \nabla f(x), \mathsf{t} \rangle = p\}, & \text{if } p > 0, \\ \{\mathsf{0}\}, & \text{if } p \leq 0. \end{cases}$$

In these conditions, we define the set

$$\mathcal{G}_x(f, \mathcal{S}) = p\, \mathsf{t}_x(\mathcal{S}),$$

as the *maximum descent set* of $f_{|\mathcal{S}}$ at x.

Let us note that even when $\mathcal{S}$ is a W-compact set, $\mathcal{G}_x(f, \mathcal{S})$ can contain a non-numerable quantity of elements. For example, if x is the vertex of a revolution half cone and $-\nabla f(x)$ points towards the interior of the cone in the direction of its axis, then $\mathsf{t}_x(\mathcal{S})$ is $\mathcal{T}_x(\mathcal{S})$.

If $x \in \mathcal{S}$, then the set

$$\mathcal{N}_x(\mathcal{S}) = \{\mathsf{q} \in S^2 : \langle \mathsf{q}, \mathsf{t} \rangle \leq 0 \text{ for each } \mathsf{t} \in \mathcal{T}_x(\mathcal{S})\},$$

can be defined as the *normal set* to $\mathcal{S}$ at x, in the sense that if $\nabla f(x) \neq \mathsf{0}$ and $-\dfrac{\nabla f(x)}{|\nabla f(x)|} \in \mathcal{N}_x(\mathcal{S})$ then x is in equilibrium on $\mathcal{S}$, and then we will say that x is a *generalized stationary point* of $f_{|\mathcal{S}}$. Let us note that if $\mathcal{T}_x(\mathcal{S})$ has only one element t, then $\mathcal{N}_x(\mathcal{S})$ is a closed hemisphere. Hence, in general, $\mathcal{N}_x(\mathcal{S})$ is the intersection of all the closed hemispheres associated to each $\mathsf{t} \in \mathcal{T}_x(\mathcal{S})$. If x belongs to a face, then $\mathcal{N}_x(\mathcal{S})$ has only two opposite points that define the normal direction to the face. In the simple case in which $\mathcal{S}$ is the boundary of a convex polyhedron, if x belongs to an edge, then $\mathcal{N}_x(\mathcal{S})$ is an arc of circumference, and if x is a vertex where r faces meet, then $\mathcal{N}_x(\mathcal{S})$ is the convex spherical r-gon whose vertices are the outer normals of these faces. In a generic case, $\mathcal{N}_x(\mathcal{S})$ can adopt multiple forms. If $\mathcal{N}_x(\mathcal{S})$ has non-null bi-dimensional measure, then x necessarily is a vertex, but no more general results exist. For example, $\mathcal{N}_x(\mathcal{S})$ can be the empty set in a vertex. The points

$x \in \mathcal{S}$ such that $\mathcal{N}_x(\mathcal{S}) = \emptyset$ have more freedom of movement than a point on a face, because x is a generalized stationary point of $f_{|\mathcal{S}}$ only when x is a stationary point of f.

For a given $x \in \mathcal{S}$, the calculation of $\mathcal{G}_x(f, \mathcal{S})$ requires in general to solve an optimization problem. However, except when x belongs to the boundary of a face C such that $\overline{C}$ is not regular at x -situation that must be solved depending on each particular case-, the resolution of this optimization problem reduces to a finite number of trivial verifications. Effectively, let us consider a point $x \in \mathcal{S}$. If x belongs to a face, then the unique element in $\mathcal{G}_x(f, \mathcal{S})$ is $-Pr_{T_x(\mathcal{S})}\nabla f(x)$; *i.e*, the projection of $-\nabla f(x)$ on the tangent plane $T_x(\mathcal{S})$. Else, let us suppose that x is a vertex belonging to the boundary of the faces $h_1, \ldots, h_r$ and of the edges $e_1, \ldots, e_s$, and that $\overline{h_j}$ are regular at x. Then, let us consider the tangent planes $\pi_j = T_x(\overline{h_j})$ of each face at x. Let $\mathtt{t}_1, \ldots, \mathtt{t}_s$ also be the unitary tangent vectors at x of each edge. Consider now the closed half straight lines $l_1, \ldots, l_s$ generated by $\mathtt{t}_1, \ldots, \mathtt{t}_s$ and the closed subsets $\hat{\pi}_j$ of each tangent plane delimited by the two half straight lines corresponding to its boundary edges. The problem reduces to finding the best approximation of $x - \nabla f(x)$ to the r sets $\hat{\pi}$ and to the m half straight lines l that do not belong to any $\hat{\pi}$. Then we can calculate $y^j = -Pr_{T_x(\overline{h_j})}\nabla f(x)$, and generate a list L with all the scalars $|y^j|$ for each j such that $x - y^j \in \hat{\pi}_j$ and with the m scalars $-\langle \nabla f(x), \mathtt{t} \rangle$ corresponding to the m half straight lines referred above. In this conditions, p is the maximum element in L, and $\mathtt{t}_x(\mathcal{S})$ is directly obtained. Other simpler cases can be solved analogously.

Returning to the Fekete points problem, for the calculation of the advance direction w, we can choose any of the elements of $\mathcal{G}_x(V_i, \mathcal{S})$ as F_i^T. On the other hand, the different definitions made above can be directly generalized. If $\mathcal{M} = \mathcal{S}^N$ and $x = \{x_1, \ldots, x_N\} \in \mathcal{M}$, then we denote the mobility set of the configuration $x \in \mathcal{M}$ by $\mathcal{T}_x(\mathcal{M}) = \mathcal{T}_{x_1}(\mathcal{S}) \times \ldots \times \mathcal{T}_{x_N}(\mathcal{S})$. The sets $\mathtt{t}_x(\mathcal{M})$, $\mathcal{G}_x(\mathcal{I}, \mathcal{M})$ and $\mathcal{N}_x(\mathcal{M})$ can be defined analogously.

5.4 The Algorithm

With the background of the precedent subsections, we can describe the main steps of our algorithm for the estimation of Fekete points in W-compact sets. We want to point out that an important part of that background has the objective of producing good initial positions to obtain true nearly optimal configurations on a non-smooth object.

The resolution process has two different parts. The first one has a purely geometric character, and it comprises the description of the W-compact set $\mathcal{S}$, the construction of its approximating regular surfaces and the choice of a procedure for projecting points from one of these objects to the other. The second part consists in an iterative algorithm for the search of Fekete points, and it includes the determination of an advance direction, a step size and a geometric criterion to return the points to the object; moreover, all these items must be reformulated when the points move on the non-smooth W-compact set.

We have presented above a useful technique for the definition of approximating implicit surfaces. In any case, independently of the procedure used for the generation of these surfaces, we must note that to obtain good initial positions it is necessary to design an *ad*

hoc approximation strategy for each considered problem, in the sense that the number of intermediate approximating surfaces and its degree of approximation to $\mathcal{S}$ must be adapted to the specific geometric difficulties of $\mathcal{S}$ and to the number of points. In the following section we present a variety of examples that show how this strategy can be developed in a simple way in many practical cases. On the other hand, the closest point technique provides a very general way of projecting points from a set to other. However, it can project two different points to the same position and it requires to solve a non-trivial optimization problem. In many cases to project along the normal direction can also be an interesting method. In general, it can be done fast by means of a one-dimensional Newton method, although it is possible that this direction does not intersect with the involved set. In any case, from our experience, any reasonable projection procedure produces in practice good results. Let us also note that any projection method has always a computational cost of order N -in each iteration-, and hence it is a minor problem. All these comments are also applicable to the return algorithm corresponding to the iterative process.

Although the descent algorithm in an approximating surface is in linear tendency, the potential energy will be far from any local minimum after the projection to the next surface. Therefore, when we are on an approximating surface, we only search configurations in a reasonably good equilibrium state. It can be sufficient to take a maximum disequilibrium degree between 10^{-2} and 10^{-3}. In these conditions, the computational cost of the process of obtaining a good initial position on $\mathcal{S}$ has low signification in comparison with the computational cost of searching a near optimal configuration on $\mathcal{S}$. For the application of the descent algorithm in $\mathcal{S}$, F_i^T must be calculated like it has been indicated in the previous subsection. However, some specific considerations must be made. If a particle moving on a face of $\mathcal{S}$ crosses its boundary, it must be projected to this boundary before F_i^T is actualized. In the new position, F_i^T will decide whether the particle will move along the boundary, will return to the original face or will go to other face. An analogous procedure must be carried out if a particle moving along an edge of $\mathcal{S}$ crosses its boundary.

We finish this section presenting a scheme of our proposal for the numerical obtention of estimations of the Fekete points of a W-compact set $\mathcal{S}$:

1. Generate a good initial configuration on $\mathcal{S}$.
   - 1.1. Definite r approximating regular surfaces S_k, $1 \leq k \leq r$.
   - 1.2. Generate a random configuration of N points on S_1.
   - 1.3. For each k, $1 \leq k \leq r$, obtain a configuration in a reasonably good equilibrium state on S_k by means of the descent algorithm and project it to the next surface. The last projection is from S_r to $\mathcal{S}$.
2. Starting from the last configuration, apply the descent algorithm to obtain a nearly optimal configuration on $\mathcal{S}$ taking into account its non-smoothness.

We want to remark that the total computational cost of the process of obtaining a nearly optimal configuration on a W-compact set $\mathcal{S}$ is essentially the same in all the cases that we have considered, and this cost seems to be less that N^3.

6 Some Examples

The following examples show the versatility of our algorithm. We have included some examples with academic interest and others of playful character, although with evident difficulties with regards to the obtaining of equilibrium configurations.

6.1 Unit Cube

For this case, we use approximating regular surfaces implicitly described by

$$f_p(x,y,z) = e^{p(x^2-0.25)} + e^{p(y^2-0.25)} + e^{p(z^2-0.25)} = 1,$$

with $p \in \mathbb{R}^+$. More explicitly, we work with two approximating surfaces defined by $p = 15, 30$, respectively.

Figure 8 illustrates the general behavior of our algorithm for non-smooth surfaces. In the upper part we show the final configurations -with a maximum disequilibrium degree of 10^{-2}- corresponding to the two approximating regular surfaces with $N = 10537$ and as we can see, to pass from the approximation with $p = 15$ to the approximation with $p = 30$ implies an important increase of the density of particles in the more curved zones, that correspond to the edges and vertices of the final cube. The projection between surfaces has been carried out along the direction of the normal vector by means of the Newton algorithm. In the same Figure (down), a near-optimal configuration on the unit cube $\mathcal{S}$ and the corresponding convergence graph are displayed. Let us note that we have not used any symmetry in this calculation. In addition, the typical convergence behavior described in Section 3 can be observed. It is clear that almost the whole second half of the convergence path is in linear tendency.

We have used this example to study the approximation process of the interior field and the electrostatic charge density of the cube by means of a sequence of Fekete N-tuples, $\{\omega_N\}_{N=2}^{\infty}$. The obtained results confirm the quality of the solutions provided by our algorithm and they agree with certain theoretical and numerical results of other authors working on these topics. For instance, Korevaar and Monterie, in the Theorem 1.2 in [11], give the following result involving the interior field. If x is a point in the interior of the solid cube, $d_x = d(x, \mathcal{S})$ and F_x^N is the field due to ω_N at x -*i.e*, the force that would act over a unitary charge on x due to N equal charges of magnitude $\dfrac{1}{N}$ located at ω_N-, then there exists a scalar c such that for each $N \geq 2$,

$$|F_x^N| \leq c\,\frac{1+d_x}{d_x^3}\,\frac{1}{\sqrt{N}}.$$

Figure 9 (up) shows the maximum value of $\dfrac{d_x^3|F_x^N|}{1+d_x}$ in the interior of the cube for different values of N covering three orders of magnitude. Each maximum is obtained by evaluating in almost 10^5 points. It must be observed that a value for the coefficient c valid for each

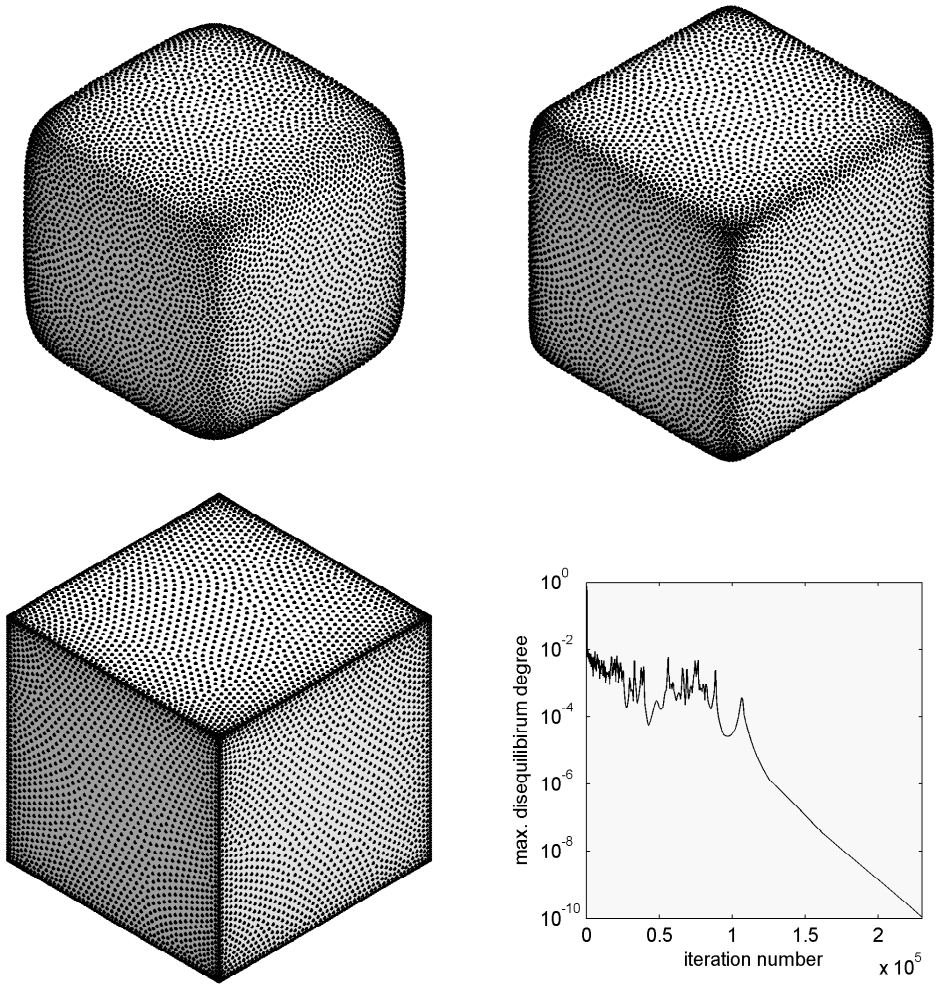

Figure 8: Approximating configurations, final near-optimal configuration and convergence of the algorithm for the problem of the Fekete points of the unit cube with $N = 10537$ and the Newtonian kernel.

N in the cube can be adjusted from the trivial case $N = 2$. However, this value would be excessively conservative for large N. For this reason, the first values of N have not been considered in the Figure. In any case, our calculations adjust sharply to the order $\frac{1}{\sqrt{N}}$. In fact, for N sufficiently large, we propose a value for the constant c of approximately $c = 0.036$.

A major open question is to obtain the electrostatic charge density of a cube. A theoretical analysis of the asymptotic behavior of the electrostatic charge density near the edges and the vertices of conductor bodies was realized by Fichera in [5]. The obtained results were applied to the unit cube in [6]. The problem has been also treated by means of different numerical techniques. In [14], for instance, the dependence of the density on the distance r from an edge for points in the middle of a face and on the distance from a vertex for points

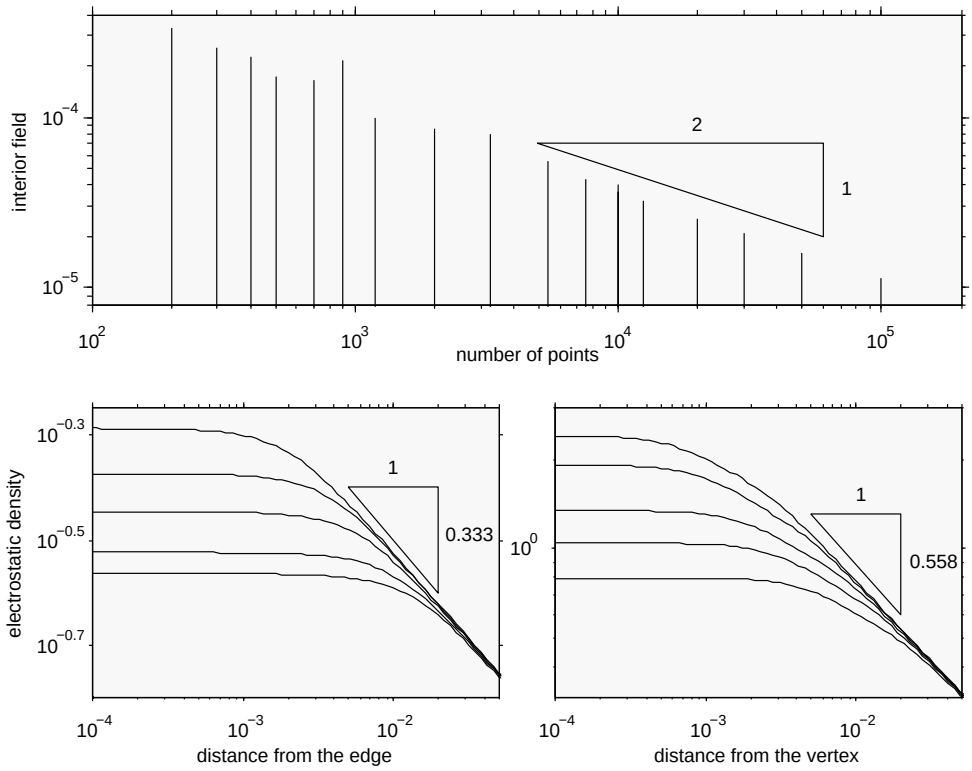

Figure 9: Approximation of the interior field and the electrostatic charge density of the unit cube by means of Fekete points.

along the diagonal of a face are considered, and numerical evidence of the fact that this dependence has the form $\alpha r^{-\frac{1}{3}}$ and $\beta r^{-0.558}$, respectively, is presented.

In Figure 9 (down) we give approximations of the electrostatic charge density near an edge and near a vertex of the unit cube for $N = 5000, 10000, 20000, 50000$ and 100000, and we compare it with the estimation given in [14]. The approximating curves have been obtained by evaluating the normal component F^n of the total force due to the N charges -of value $\frac{1}{N}$- at points on $\mathcal{S}$ located in the middle of a face and along a diagonal. The values of the density presented are $\frac{|F^n|}{2\pi}$. The density given by the Fekete points tends, although very slowly, to the estimations that appear in the literature. We want to note here that the objective of this study is to evaluate the suitability of the configurations obtained with our algorithm, and not to carry out an accurate asymptotic analysis of the electrostatic charge density of the cube.

6.2 Kelvin Polyhedron

With this example we want to analyze some indicators of the symmetry and the proportionality of the configurations obtained with our algorithm. In that sense, the Archimedean Kelvin Polyhedron has an interesting geometry.

The approximating surfaces have been constructed by combining separately the planes corresponding to the different faces. We used the following implicit expression

$$\begin{aligned} f_p(x,y,z) = {} & e^{p(x-0.5)} + e^{p(y-0.5)} + e^{p(z-0.5)} + e^{-p(x+0.5)} + e^{-p(y+0.5)} + e^{-p(z+0.5)} \\ & + e^{p(x+y+z-0.75)} + e^{p(-x+y+z-0.75)} + e^{p(x-y+z-0.75)} + e^{p(-x-y+z-0.75)} \\ & + e^{p(x+y-z-0.75)} + e^{p(-x+y-z-0.75)} + e^{p(x-y-z-0.75)} + e^{p(-x-y-z-0.75)} = 1 \end{aligned}$$

with $p = 25,\, 60$.

Figure 10 shows a configuration of 10000 points on the Kelvin Polyhedron in linear tendency. In Table 2 we present the evolution of three ratios, r_1, r_2 and r_3, involving the number of points belonging to different faces of the polyhedron. If n_s^i, with $i = 1, \ldots, 6$, denote the number of points belonging to each square and n_h^j, $j = 1, \ldots, 8$, represent the number of points belonging to each hexagon, then $r_1 = \min \dfrac{n_s^i}{n_s^j}$, $r_2 = \min \dfrac{n_h^i}{n_h^j}$ and $r_3 = \min \dfrac{n_h^i}{n_s^j}$.

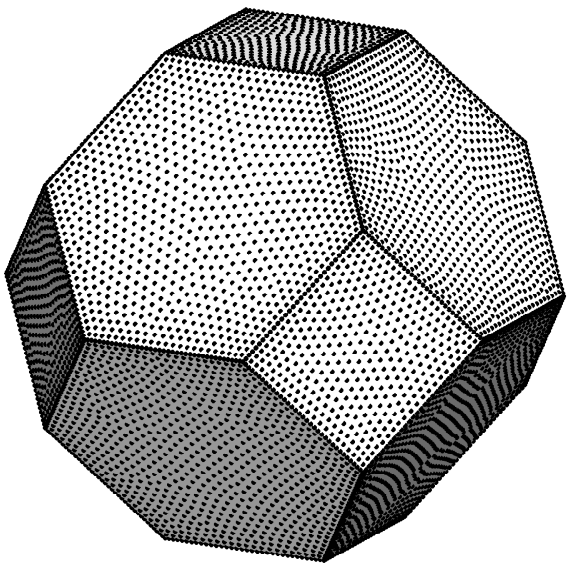

Figure 10: A near-optimal configuration on the Kelvin Polyhedron for $N = 10000$ with the Newtonian kernel.

Table 2 also includes the evolution of the charge recovered by integrating the electrostatic density given by the Fekete points. In this case, a continuum estimation of the electrostatic density has been constructed from the Delaunay triangulation associated to the points in

each face. The density value on each point x_i has been calculated as $\dfrac{|F_i|}{2\pi N}$, and these values have been linearly interpolated in each triangle. Let us note that, in spite of that this approach is very simple, the charge recovered for the distribution of 100000 points is more than the 99%.

N	r_1	r_2	r_3	q
5000	0.9884	0.9852	2.0618	0.9713
10000	0.9919	0.9923	2.0994	0.9788
20000	0.9947	0.9956	2.1300	0.9840
50000	0.9982	0.9986	2.1669	0.9893
100000	0.9984	0.9989	2.1816	0.9922

Table 2: Geometrical ratios and charge recovered.

6.3 A More General Example

Let us consider the sphere, the filled square and the curve respectively defined by

$$A = \left\{(x,y,z) \in \mathbb{R}^3 : (x-0.75)^2 + (y-0.75)^2 + (z+0.2)^2 = 0.64\right\},$$
$$B = \left\{(x,y,z) \in \mathbb{R}^3 : max\{|x|,|y|\} \leq 1,\ z = 0\right\},$$
$$C = \left\{(x,y,z) \in \mathbb{R}^3 : max\{|x-0.5|,|z|\} = 0.5,\ y = -0.5\right\}.$$

We analyze here the Fekete points problem for the W-compact set $\mathcal{S} = A \cup B \cup C$. This example combines the three cases presented in Subsection 5.2; *i.e*, a surface boundary of an open set, a surface with boundary and a curve.

It must be taken into account that the electrostatic charge density in the part of B inside of the sphere A, that we denote by D, is necessarily null. For this reason, it is not necessary consider D when the Newtonian kernel is used. In fact, we have carried out some numerical experimentation with this kernel including D in the set $\mathcal{S}$, and we have observed that, effectively, the particles leave D. On the other hand, D must be explicitly included in $\mathcal{S}$ when other kernels are considered, and then the approximating surfaces require to be connected in a way similar to the one indicated in Subsection 5.1.

For the construction of the approximating surfaces, we have used the following implicit

functions,

$$f_1(x,y,z) = e^{2p(x^2-1)} + e^{2p(y^2-1)} - 1,\ \ f_2(x,y,z) = e^{2pz} - 1,$$

$$f_3(x,y,z) = (x-0.75)^2 + (y-0.75)^2 + (z+0.2)^2 - 0.64,$$

$$f_4(x,y,z) = e^{pf_3(x,y,z)} - 1,\ \ f_5(x,y,z) = e^{2p(x+0.5)^2-0.25} + e^{2pz^2-0.25} - 1,$$

$$f_6(x,y,z) = e^{2p(y+0.5)} - 1,\ \ f_7(x,y,z) = (x-h)^2 + (y-h)^2 + z^2,$$

where $h = 0.75 - \sqrt{0.3}$.

In these conditions, the implicit expression of the approximating surfaces used when D is not considered is

$$f_p(x,y,z) = e^{-pf_2^2(x,y,z)+f_1(x,y,z)} + e^{-pf_3(x,y,z)} + e^{-p(f_6^2(x,y,z)+f_5^2(x,y,z))+1} = 1.$$

If D is included in the analysis, the corresponding expression is

$$f_p(x,y,z) = \frac{1}{e^{-pf_2^2(x,y,z)+f_1(x,y,z)} + e^{-pf_4^2(x,y,z)+1} + e^{-p(f_6^2(x,y,z)+f_5^2(x,y,z))+1}} + e^{-3pf_7(x,y,z)+1} = 1.$$

Figure 11 shows a good configuration of 2000 points on $\mathcal{S}$. The effect of connecting conductor bodies of different dimension can be observed. The repulsion of the sphere predominates over the repulsion of the square, and also the repulsion of the square predominates over the repulsion of the curve.

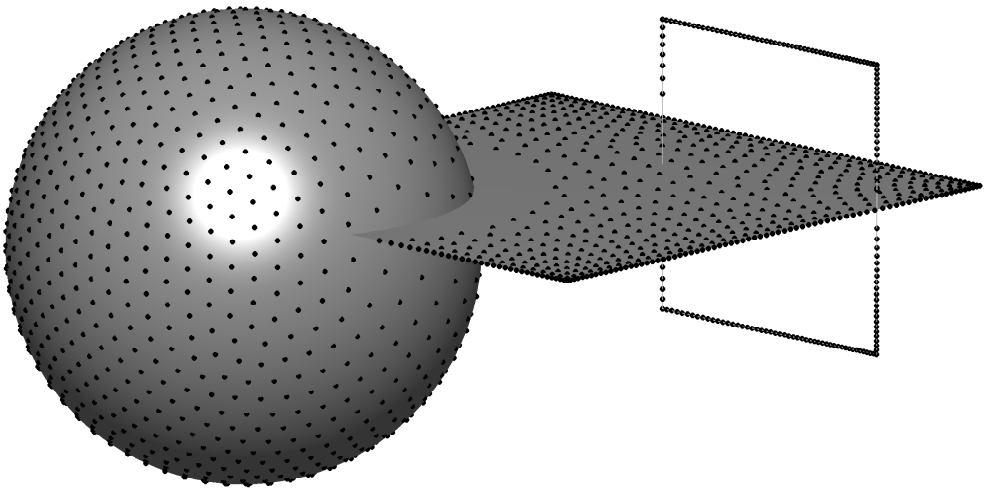

Figure 11: Good configuration of $N = 2000$ points on $\mathcal{S}$ for the Newtonian kernel.

It is important to note that in the approximation process corresponding to this case an object with parts of different dimension is being covered by a single surface. It requires to be specially careful with regards to the control of the local degree of approximation in each one of these parts. In this exercise we have used the approximating surfaces obtained taking $p = 13.5, 15$ in the above expression.

6.4 A Still Life

We want to conclude this paper presenting a funny exercise that shows the adaptability of the proposed technique to a great variety of geometries. We have composed a still life with near-optimal configurations for the Newtonian kernel of 1500 points on a whole apple, 2500 points on a bitten apple and 1500 points on a Canary banana. The three objects have been treated individually, although we present all them in the same Figure 12.

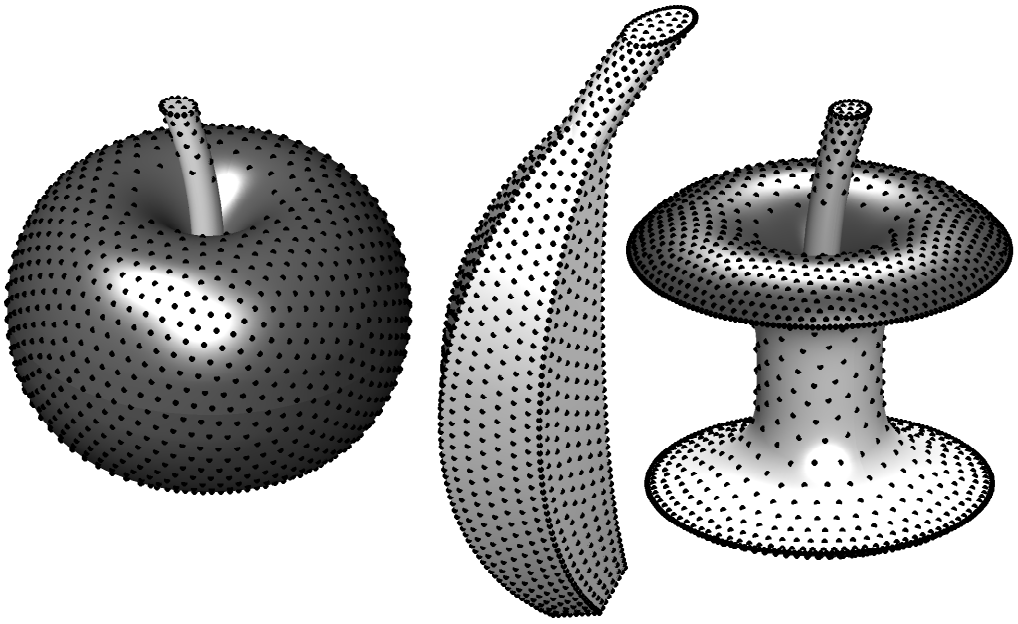

Figure 12: A Newtonian still life.

The approximating surfaces of the apples are based in the following implicit functions,

$$
\begin{aligned}
f_1(x,y,z) &= \left(\frac{\sqrt{x^2+y^2}-1.5}{1.4}\right)^2 + \left(\frac{z-0.15}{2}\right)^2 - 1,\\
f_2(x,y,z) &= \sqrt{x^2+y^2} - 1.6\left(\frac{z}{1.65}\right)^4 - 0.8,\\
f_3(x,y,z) &= x^2 + \left(\sqrt{(y-7)^2+(z-1)^2}-7\right)^2 - r^2,\\
f_4(x,y,z) &= x^2+y^2+(z+1)^2 - 0.36,
\end{aligned}
$$

where $r = 1.5 - 1.4\sqrt{0.819375}$.

The implicit equations of the approximating surfaces for the whole apple and for the bitten apple are respectively

$$
f_p(x,y,z) = e^{-pf_1(x,y,z)} + e^{-pf_4(x,y,z)} + \frac{1}{e^{1.5pf_3(x,y,z)} + e^{-1.5pz} + e^{1.5p(z-3.5)}} = 1
$$

and

$$f_p(x,y,z) = \frac{1}{e^{pf_1(x,y,z)} + e^{pf_2(x,y,z)}} + e^{-pf_4(x,y,z)} + \frac{1}{e^{1.5pf_3(x,y,z)} + e^{-1.5pz} + e^{1.5p(z-3.5)}} = 1.$$

For the Canary banana, the corresponding implicit expression is

$$f_p(x,y,z) = \frac{1}{\sum_{i=1}^{5} e^{pf_i(x,y,z)} + e^{-p(\sin(0.175\pi)x + \cos(0.175\pi)z)}} + \frac{1}{e^{pf_6(x,y,z)} + e^{-pz} + e^{p(z-4)}} = 1,$$

where, for each $i = 1, \ldots, 5$,

$$f_i(x,y,z) = \cos\left(\frac{2\pi i}{5}\right)\left(5 - \sqrt{x^2+z^2}\right) - \sin\left(\frac{2\pi i}{5}\right) y + 0.75\left(\frac{16}{\pi^2}\arctan^2\left(\frac{z}{x}\right) - 1\right)$$

and $f_6(x,y,z) = y^2 + \left(\sqrt{x^2+z^2} - 5\right)^2 - 0.125$.

Acknowledgements

The authors express their sincere gratitude to Professor Antonio Gens by his unconditional support. This work has been partially supported by the CICYT under project BFM2003-06014.

References

[1] M. Atiyah and P. Sutcliffe, The geometry of points particles, *R. Soc. Lond. Proc. Ser. A Math. Phys. Eng. Sci.*, **458** (2002), 1089-1115.

[2] M. Atiyah and P. Sutcliffe, Polyedra in Physics, Chemistry and Geometry, *Milan J. Math.*, **71** (2003), 33-58.

[3] E. Bendito and A. M. Encinas, Minimizing energy on locally compact spaces: existence and approximation, *Numer. Funct. Anal. and Optimiz.*, **17 (9-10)** (1996), 843-865.

[4] J. F. Blinn, A generalization of algebraic surface drawing, *ACM Transactions on Graphics*, **1** (1982), 235-256.

[5] G. Fichera, Comportamento asintotico del campo elettrico e della densita elettrica in prossimita dei punto singolari della superficie conduttore, *Rendiconti del Seminario Matematico dell'Universita e del Politecnico di Torino*, **32** (1973-1974), 111-143.

[6] G. Fichera and M. A. Sneider Ludovici, Distribution de la charge électrique dans le voisinage des sommets et des arêtes d'un cube, *C. R. Acad. Sc. Paris*, **278 (A)** (1974), 1303-1306.

[7] B. Fuglede, On the Theory of Potentials in locally compact spaces, *Acta Math.*, **103** (1960), 139-215.

[8] F.X. Giraldo, T. Warburton, A nodal triangle-based spectral element method for the shallow water equation on the sphere, *Journal of Computational Phisycs*, **207** (2005), 129-150.

[9] D.P. Hardin and E.B. Saff, Discretizing manifolds via minimum energy points, *Notices Amer. Math. Soc.*, **51** (2004), 1186-1194.

[10] W. Heinrichs, Improved Lebesgue constants on the triangle, *Journal of Computational Phisycs*, **207** (2005), 625-638.

[11] J. Korevaar and M.A. Monterie, Approximation of the equilibrium distribution by distributions of equal point charges with minimal energy, *Trans. Amer. Math. Soc.*, **350** (1998), 2329-2348.

[12] A.B.J. Kuijlaars and E.B. Saff, Asymptotics for minimal discrete energy on the sphere, *Trans. Amer. Math. Soc.*, **350** (1998), 523-538.

[13] N.S. Landkof, *Foundations of modern Potential Theory*, Springer-Verlag, (1972).

[14] M. Mascagni and N. A. Simonov, The random walk on the boundary method for calculating capacitance, *Journal of Computational Physics*, **195** (2004) 465-473.

[15] K.J. Nurmela, Constructing spherical codes by global optimization methods, *Helsinki University of Technology, Series A: Research Reports*, **32** (1995).

[16] P.O. Persson and G. Strang, A simple mesh generator in MATLAB, *SIAM Review*, **46 (2)** (2004), 329-345.

[17] E.A. Rakhmanov, E.B. Saff and Y. Zhou, Minimal discrete energy on the sphere, *Math. Res. Lett.*, **1** (1994), 647-662.

[18] E.B. Saff and A.B.J. Kuijlaars, Distributing many points on a sphere, *Math. Intelligencer*, **19** (1997), 5-11.

[19] K. Shimada and D.C. Gossard, Automatic triangular mesh generation of trimmed parametric surfaces for finite element analysis, *Computer Aided Geometric Design*, **15** (1998), 199-222.

[20] S. Smale, Mathematical problems for the next century, *Math. Intelligencer*, **20** (1998), 7-15.

[21] M.A. Taylor, B.A. Wingate and R.E. Vincent, An algorithm for computing Fekete points in the triangle, *SIAM J. Numer. Anal.*, **38** (2000), 1707-1720.

[22] A. Witkin and P. Heckbert, Using particles to sample and control implicit surfaces, *Computer Graphics Proc. SIGGRAPH 94*, (1994), 269-278.

[23] Y. Zhou, *Arrangements of points on the sphere*, Ph.D. Department of Mathematics, University of South Florida, (1995).